IOPscience iopscience.iop.org

Home Search Collections Journals About Contact us My IOPscience

Versatile theranostics agents designed by coating ferrite nanoparticles with biocompatible polymers

This content has been downloaded from IOPscience. Please scroll down to see the full text.

2016 Nanotechnology 27 255702

(http://iopscience.iop.org/0957-4484/27/25/255702)

View the table of contents for this issue, or go to the journal homepage for more

Download details:

IP Address: 144.173.6.37
This content was downloaded on 01/06/2016 at 06:08

Please note that terms and conditions apply.

IOP Publishing Nanotechnology
Nanotechnology 27 (2016) 255702 (12pp) doi:10.1088/0957-4484/27/25/255702

Versatile theranostics agents designed by coating ferrite nanoparticles with biocompatible polymers

M Zahraei[1], M Marciello[2], A Lazaro-Carrillo[3], A Villanueva[3,4], F Herranz[5], M Talelli[6], R Costo[2], A Monshi[1], D Shahbazi-Gahrouei[7], M Amirnasr[8], B Behdadfar[1] and M P Morales[2]

[1] Department of Materials Engineering, Isfahan University of Technology, Isfahan 84156-83111, Iran
[2] Department of Biomaterials and Bioinspired Materials, Materials Science Institute of Madrid (ICMM)/CSIC, Sor Juana Inés de la Cruz 3, Cantoblanco, 28049 Madrid, Spain
[3] Department of Biology, Universidad Autónoma de Madrid, Cantoblanco, 28049 Madrid, Spain
[4] Instituto Madrileño de Estudios Avanzados en Nanociencia (IMDEA Nanociencia), Cantoblanco, 28049 Madrid, Spain
[5] Advanced Imaging Unit, National Center for Cardiovascular Research (CNIC) and CIBERES, Melchor Fernández Almagro 3, 28029 Madrid, Spain
[6] Department of Immunology and Oncology and NanoBiomedicine Initiative, National Centre of Biotechnology (CNB)/CSIC, Darwin 3, Cantoblanco, 28049 Madrid, Spain
[7] Department of Medical Physics, School of Medicine, Isfahan University of Medical Sciences, Isfahan 81746-734615, Iran
[8] Department of Chemistry, Isfahan University of Technology, Isfahan 84156-83111, Iran

E-mail: marziamarciello@gmail.com and shahbazi@med.mui.ac.ir

Received 22 October 2015, revised 25 February 2016
Accepted for publication 14 March 2016
Published 17 May 2016

Abstract

Three biocompatible polymers, polyethylene glycol (PEG), dextran and chitosan, have been used in this work to control the colloidal stability of magnetic nanoparticles (14 ± 5 nm in diameter) and to vary the aggregation state in order to study their effect on relaxometric and heating properties. Two different coating strategies have been deeply developed; one based on the formation of an amide bond between citric acid coated nanoparticles (NPs) and amine groups present on the polymer surface and the other based on the NP encapsulation. Relaxometric properties revealed that proton relaxation rates strongly depend on the coating layer hydrophilicity and the aggregation state of the particles due to the presence of magnetic interactions. Thus, while PEG coating reduces particle aggregation by increasing inter-particle spacing leading to reduction of both T_1 and T_2 relaxation, dextran and chitosan lead to an increase mainly in T_2 values due to the aggregation of particles in bigger clusters where they are in close contact. Dextran and chitosan coated NPs have also shown a remarkable heating effect during the application of an alternating magnetic field. They have proved to be potential candidates as theranostic agents for cancer diagnosis and treatment. Finally, cytotoxicity of PEG conjugated NPs, which seem to be ideal for intravenous administration because of their small hydrodynamic size, was investigated resulting in high cell viability even at 0.2 mg Fe ml^{-1} after 24 h of incubation. This suspension can be used as drug/biomolecule carrier for *in vivo* applications.

S Online supplementary data available from stacks.iop.org/NANO/27/255702/mmedia

Keywords: Mn Zn ferrite, coating strategies, biocompatible polymer, biomedicine, theranostic agents, HeLa cell culture

 © 2016 IOP Publishing Ltd Printed in the UK

(Some figures may appear in colour only in the online journal)

1. Introduction

Spinel ferrites nanoparticles, MFe_2O_4 (M = Mn, Fe, Co, etc), are among the most interesting magnetic nanomaterials due to their potential for important biotechnological applications in catalysis, biomolecule separation, medical diagnosis and treatment etc [1–3]. The main advantage of these ferrites is their ability to change their magnetic properties on varying the proportions of their constituents [4, 5]. In the case of biomedical applications, it is particularly important to develop nanoparticles (NPs) with tunable magnetism that is superparamagnetic behavior at RT (zero coercivity and remanence) and high saturation magnetization (M_s) values, which are strongly dependent on the core nature, size and their monodispersity. For example, it was demonstrated that manganese- or cobalt- doped ferrite NPs have tunable magnetic characteristics and significantly enhanced MRI contrast effect with respect to conventional iron oxide NPs [6, 7]. This enhancement is significant for clinical purposes because the probe dosage level can be progressively lowered when NPs with improved contrast enhancement effects are employed [6]. Manganese zinc ferrite (MZF) NPs prepared by thermal decomposition have been demonstrated to act as powerful negative contrast agents [6]. Moreover, these NPs have recently gained interest as magnetic hyperthermia agents due to the tunability of their magnetic properties by varying the proportions of Mn and Zn ions in their structure [8, 9].

For biomedical applications, NPs must be coated with biocompatible molecules or polymers, such as polyethylene glycol (PEG) [10], dextran [11–13], chitosan [14–16], polyethylenimine (PEI) [17], and phospholipids [18] that have been demonstrated to stabilize magnetic nanoparticles (MNPs) under physiological conditions. PEG, dextran and chitosan are particularly interesting because they are non-toxic, biocompatible and can prolong the MNPs' life-time in the blood [14, 19]. Dextran has been widely used to coat superparamagnetic iron oxide NPs (SPION) because of its polar interactions (chelation and hydrogen bonding) that provide high affinity for iron oxide NP surfaces [20]. So many of the commercial ferrofluids are dextran coated SPION [21]. In the literature, different methods to attach dextran to the MNP surface are described [13, 21, 22], however, covalent bonds are preferred for their enhanced stability in physiological conditions [13, 23]. PEG is a biocompatible linear synthetic polyether that can be prepared with a wide range of sizes and terminal functional groups [21]. The uncharged, extremely hydrophilic nature of PEG, combined with its low toxicity and low immunogenicity, render these PEG-coated NP 'invisible' to the immune system making them attractive for biomedical applications [10]. PEG is commonly used in many drug and gene delivery applications because it reduces the adsorption of blood reticuloendothelial system factors to the NP surface and NP clearance by cells of the mononuclear phagocytic system [24].

On the other hand, chitosan is a unique cationic, hydrophilic polymer that has beneficial properties such as low immunogenicity, excellent biodegradability as well as a high positive charge that easily forms polyelectrolyte complexes with negatively charged entities [22]. Magnetite–chitosan NPs have been obtained by crosslinking chitosan amino groups using glutaraldehyde [14, 15]. The disadvantage of this method is the toxicity of this cross-linker [16]. In contrast, ionic gelation (polyionic coacervation) is an interesting technique that uses non-toxic polyanions, such as sodium tripolyphosphate (TPP) as ionic crosslinker. This procedure is simple and reproducible and NPs are encapsulated in a chitosan shell by ionic interactions [16].

In this study, Mn-Zn ferrite (MZF) NPs have been prepared using a direct, efficient and environmentally friendly hydrothermal method. Coating strategies using biocompatible polymers have been deeply and successfully developed for this type of particle. As a consequence biocompatible and robust NPs with physicochemical properties suitable for bioapplications were obtained and compared. In more detail, MZF NPs were coated with PEG (P), dextran (D) and chitosan (Ch) by using strong interactions polymer-MNPs. As a first approach the three polymers were anchored to the negatively charged NPs surface (due to the presence of citric acid carboxylic groups) via carbodiimide chemistry with the formation of an amide bond. In the case in which the considered strategy was not satisfactory, a second procedure consisting of NP encapsulation by ionic gelation technique was used. The success of the coating was followed by electrophoretic measurements, infrared (IR) and thermogravimetric analysis (TGA). Moreover, to study the efficiency of these polymer coated NPs as biomedical agents in MRI and magnetic hyperthermia therapy, the effects of NP suspension were investigated by NMR relaxometry and SAR measurements.

2. Experimental section

2.1. Materials

Chemical materials, including $FeCl_3 \cdot 6H_2O$, $ZnCl_2$, $MnCl_2 \cdot 4H_2O$, nitric acid (HNO_3), iron III nitrate ($Fe(NO_3)_3$), sodium hydroxide (NaOH) and hydrochloric acid (HCl) were purchased from Merck Co. in high purity. PEG-NH_2 (methoxypolyethelene glycol amine) with a molecular weight of 20 kDa and low molecular weight chitosan (degree of deacetylation = 86.6%) were commercial products provided by Fluka Co. All other chemicals, including carboxymethyl dextran with a molecular weight of 12 kDa, ethylenediamine (EDA), sodium tripolyphosphate (TPP), 1-ethyl-3-(3dimethylaminopropyl)-carbodiimide hydrochloride (EDC) and N-hydroxysuccinimide (NHS) were purchased from Sigma Aldrich Co. The water used in all experiments was double distilled (ultrapure water).

2.2. NPs synthesis and surface modification

MZF NPs with size of 14 nm were synthesized by hydrothermal method as described in our previous work [25]. Briefly, stoichiometric amounts of $FeCl_3 \cdot 6H_2O$, $ZnCl_2$ and $MnCl_2 \cdot 4H_2O$ were completely dissolved in 25 ml distilled water to achieve 0.08, 0.11 and 0.17 molar concentration respectively. After 15 min stirring, a solution of NH_4OH 25% was added slowly to the medium to adjust the pH at 9.5. Vigorous stirring continued for another 10 min and a reddish brown slurry was formed. The mixed solution was poured into a Teflon lined stainless-steel autoclave (500 ml). Hydrothermal treatment was done at 180 °C for 12 h. The precipitate was washed with deionized water via magnetic decantation several times and then dried at 50 °C for 4 h.

To improve their size monodispersivity, crystallinity and activate their surface, the sample was subjected to an acid treatment [26]. Briefly, 1 ml of HNO_3 (2 M) was added to 50 mg of dried sample and the suspension was magnetically stirred for 15 min. Then, 1 ml of $Fe(NO_3)_3$ (1 M) and 3 ml of water were added, and the mixture was boiled under reflux for 30 min. When the sample was cool, an additional 1 ml of HNO_3 (2 M) was added and the sample was treated under magnetic stirring for another 15 min. The last step consisted of washing the sample three times with acetone to remove the excess acid. The resulting NPs are abbreviated as T-MZF in the text.

T-MZF NPs were coated with citric acid [27] providing the carboxylic groups necessary for the formation of an amide group with the amines present on the polymers. Briefly, 1 ml of the NP suspension (2 mg ml^{-1}) was incubated within 4 ml of citric acid solution 0.1 M at 80 °C during 30 min. The reaction product containing excess of citric acid was dialyzed against water in a 12–14 kD cut-off cellulose membrane for 48 h. NPs stabilized with citric acid are abbreviated as C-MZF.

2.3. Chemical amination of dextran

Carboxylic groups of a commercial carboxymethyl dextran were modified by using EDC and EDA as described in the literature [28] to generate amines on its surface. Briefly, 0.1 g of carboxymethyl dextran was added to 10 ml of aqueous ethylenediamine (1 M) at pH 4.75, under mechanical stirring. Solid EDC 10 mM was added to the suspension controlling that the final pH was 4.75. After 120 min of gentle stirring, the aminated polymer was dialyzed against water in a 50 kD cut-off cellulose membrane for 48 h to remove the undesirable products.

2.4. Polymer conjugation

PEG, dextran and chitosan were covalently anchored to carboxyl groups of the NPs surface through their amine group via EDC chemistry.

C-MZF NPs were suspended in 5 ml of deionized water to obtain a concentration of 2 mg ml^{-1}. Then, NHS 0.1 M and EDC 20 mM were added to C-MZF NPs suspension and mixed during 60 min to activate the carboxylic groups. After this time the suspension was centrifuged. Then the supernatant was removed and replaced with polymer solution in a molar ratio 1.5:1 (amine/carboxylic group). The mixture was adjusted to pH 7.8 by addition of NaOH. The suspension was stirred for 18 h at room temperature followed by extensive dialysis (cut-off: 50 and 100 kDa). NPs coated with PEG and dextran are abbreviated as P-MZF, D-MZF respectively.

2.5. Encapsulation by chitosan

Naked NPs were encapsulated in a chitosan shell by ionotropic gelation technique based on the interaction between the positively charged amino groups of chitosan and negatively charged phosphate groups of TPP.

A chitosan solution was prepared by dissolving chitosan in 0.1% w/v HCl solution until the solution was transparent. The MZF NPs suspension (3 mg ml^{-1}) was first mixed with 3 ml of chitosan solution (1 mg ml^{-1} chitosan in 0.1% w/v HCl) and the reaction mixture was vigorously stirred for 15 min.

Different amounts of TPP (0.89, 1.39, 1.25 and 1.67 mg ml^{-1}) were dissolved in deionized water and added to Ch solution to find the right concentration that permitted the spontaneous formation of Ch coated MZF NPs (Ch-MZF NPs). The appropriate amount of TPP is important because a higher amount led to flocculation indicating NPs precipitation while lower amounts did not permit NPs formation. To promote crosslinking, mild magnetic stirring at room temperature continued for 30 min. Then, to remove excess unbounded chitosan and TPP, the resulting particles were washed several times by centrifugation and redispersion of precipitates in distilled water. For powder characterizations, the precipitate was freeze dried at −70 °C and at pressure of 0.2 mbar.

2.6. Characterization

Phase identification was carried out using a Bruker D8ADVANCED model diffractometer, with CuKα radiation ($\lambda = 1.5406$ A). Scherrer's formula ($d = 0.9\lambda/B\cos\theta$) was used to estimate the mean crystallite size (d) of the samples with full-width at half-maximum value (β) obtained from the spinel peaks [29]. Elemental analysis (ICP-OES) was used to quantify Mn, Zn and Fe in the final composition of the ferrites. Samples were first digested with nitro-hydrochloridric acid.

Particle and aggregation size were determined from TEM micrographs using a 200 keV JEOL-2000FXII microscope. For the observation of the sample in the microscope, a drop of diluted magnetic NPs suspension in water was placed on a carbon-coated copper grid. The mean particle size distribution was evaluated by measuring the largest internal dimension of at least 100 particles. Afterward, data were fitted to a log normal distribution by obtaining the mean size. Colloidal properties were characterized by dynamic light scattering (DLS) using a Malvern instrument Zetasizer (DTS Version 5.02) and 0.5 mM Fe NPs suspensions in water. Z-average values in intensity at pH 7 were used as mean hydrodynamic size (D_H), and the Z potential was measured in a 0.01 M

KNO_3 solution. HNO_3 or KOH was added to the solution to alter the pH. Fourier transform infrared spectroscopy (FTIR) spectra were acquired using a Nicolet 20 SXC FTIR to confirm the ferrite phase, the nature of the coating and its surface bonding. IR spectra of the magnetic NPs were recorded between 4000 and 250 cm^{-1}. Samples were prepared by pressing the ferrite powder at 2% in KBr into pellets. TGA was carried out in a Seiko TG/DTA 320U, SSC5200 to determine the weight percentage of polymer in the coated NPs. The analysis was performed from room temperature to 1000 °C with an air flow. The magnetic properties of the samples were recorded in a vibrating sample magnetometer (Mag Lab VSM, Oxford Instrument). Hysteresis loops of the powder samples (pressed in a pellet) were measured at room temperature (RT) and 5 K at the rate of 5 kOe · min^{-1}. The saturation magnetization was evaluated by extrapolating the experimental data obtained in the high-field range to an infinite field; in the high-field range, the magnetization increases linearly with H, which can be approximated to a $1/H$ law.

In order to evaluate the efficiency of the hydrophilic suspensions as contrast agents, relaxation time measurements were carried out in a MINISPEC MQ60 (Bruker) at 37 °C and a magnetic field of 1.5 T. The preparation of the samples involves the solidification of the hydrophilic suspensions in agar solution (4%) with different concentrations. The relaxivities values ($r_{1,2}$, s^{-1} mM^{-1}) were calculated by the liner fitting of the relaxation rates $R_{1,2}$ ($1/T_{1,2}$, s^{-1}) values for each Fe concentration and blank solution, according to equation (1):

$$R_{1,2} = R^{\circ}_{1,2} + r_{1,2}\,[\mathrm{Fe}] \tag{1}$$

where $R^{\circ}_{1,2}$ (s^{-1}) is the relaxation rate in the absence of contrast agent, [Fe] is the contrast agent concentration (mM) and and $r_{1,2}$ (s^{-1} mM^{-1}) is the relaxivity [30].

To measure the heating capacity of the ferrofluids under an alternating magnetic field, 150 μl of each dispersion was placed in an eppendorf and positioned in the induction coil. Next, an alternating magnetic field was applied, with a frequency of 250 kHz and a magnetic field amplitude of 25 kA m^{-1}, while the sample temperature was monitored using a non-contact infrared thermometer. The coil temperature was controlled at 31 °C. The temperature rise of the sample with respect to time was recorded, and from the slope of the heating curve ($\Delta T/\Delta t$) the specific adsorption rate was calculated using the following formula (equation (2)) [31]:

$$SAR = \frac{C_s}{m_{\mathrm{Fe}}} \cdot \left(m_{\mathrm{Fe}} \frac{\Delta T}{\Delta t} \right) \tag{2}$$

where C_s is the heating capacity of water (4.181 J $g^{-1}K^{-1}$), m_{Fe} the mass of iron in the dispersion and m_{FF} the mass of the ferrofluid.

2.7. Cell culture

Human cervix adenocarcinoma HeLa cells (ATCC® CCL-2™) were cultured as monolayers in Dulbecco's modified Eagle medium with 50 U ml^{-1} penicillin, 50 μg ml^{-1} streptomycin and 10% fetal bovine serum, in a humidified SteriCult 200 (Hucoa Erloss) incubator (37 °C, 5% CO_2). All products were purchased from Gibco and sterilized by means of 0.22 m filters (Millipore). For experiments, cells were seeded in 24-well plates (1.2×10^4 cells $well^{-1}$) and treatment was initiated 3 days after plating (~50% confluence). For some experiments, cells were seeded on 10 mm square glass coverslips placed on each well. Prussian blue staining was used to identify NP presence and location and cellular morphology after NP incubation. HeLa cells were incubated 24 h with 0.1 and 0.2 mg Fe ml^{-1} of NPs, then cells were fixed in ice-cold methanol (5 min) and incubated 15 min with an equal volume of 4% HCl and 4% $K_4[Fe(CN)_6] \cdot 3H_2O$ (all Panreac Química). Cells were washed with distilled water, counterstained with 0.5% neutral red (Panreac Química) (3 min), washed again and then air-dried. Finally they were mounted in DePeX (Serva) to be visualized and photographed in an Olympus BX61 optical microscope in bright field with an Olympus DP50 digital camera (Olympus) and processed using Adobe Photoshop 7.0 software (Adobe Systems).

Mammalian cell cultures are fundamental first line tools to assess the therapeutic efficiency and safety of new nanoparticles and provide essential information to understand cell-nanoparticle interactions. HeLa cells have been chosen because they are often used to check nano-cytotoxicity (nanomaterial cytotoxicity is composition, size, and cell type dependent) and therefore allow direct comparison with published results.

2.8. Cytotoxicity assay

HeLa cell viability was determined by the AlamarBlue assay (Invitrogen). Cells were cultured in 96-well plates (3000 cells $well^{-1}$) with various concentrations of NPs (0.1 and 0.2 mg Fe ml^{-1}) for 24 h. Cell viability was evaluated immediately or 48 h after treatment. Alamar Blue reagent was added to each well (at a concentration of 100 μl ml^{-1} in complete medium), and incubated at 37 °C for 4 h. Fluorescence was evaluated on a plate reader Synergy HT (BioTek) (530 nm excitation wavelength, 590 nm emission wavelength). Cell survival was expressed as the percentage of fluorescence of treated cells in comparison with that of control cells (without incubation with NPs). Data corresponded to mean values ± standard deviation from at least five different experiments.

3. Results and discussion

3.1. Surface modification of MZF NPs

Ferrite nanoparticles prepared in this work consist of manganese zinc ferrites with a mean size of 14 nm and a standard deviation of 5 nm. Figure 1 shows x-ray diffraction patterns of synthesized NPs before (MZF) and after (T-MZF) the acid treatment. The sample MZF presents broad peaks typical of small particles. After acid treatment (T-MZF), the peaks were slightly sharper according to a reduction in polydispersity.

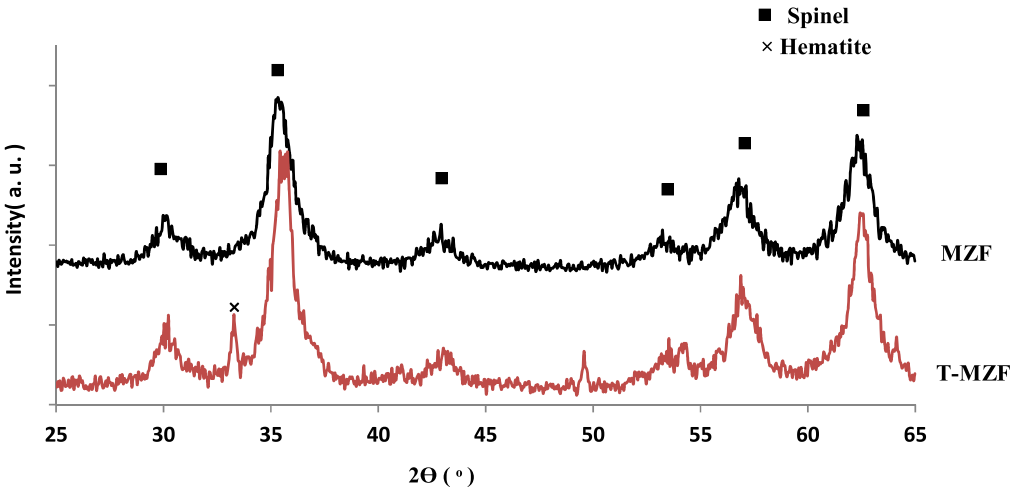

Figure 1. XRD diffraction patterns of synthesized NPs before (MZF) and after (T-MZF) acid treatment.

Table 1. Elemental ratios for MZF NPs in comparison with theoretical stoichiometric ratios before and after acid treatment.

$Mn_{0.6}Zn_{0.4}Fe_2O_4$	Mn/Zn	Mn/Fe	Zn/Fe
Stoichiometric amounts	1.50	0.30	0.20
MZF	1.23	0.30	0.24
T-MZF	0.79	0.10	0.13

Moreover, the crystalline size was reduced by the acidic treatment from 18 to 17 nm. Besides, a small peak at around 33 (2θ) can be assigned to some hematite impurities in sample T-MZF.

Table 1 shows the elemental ratios of Mn, Zn and Fe for MZF NPs in comparison with theoretical stoichiometric ratios before and after acidic treatment. For T-MZF NPs a loss in Mn and Zn content is evident (the amount of Mn and Zn was reduced to half the stoichiometric values for MnZn ferrite) probably due to the presence of these elements at the MNPs surface.

After acidic treatment MZF NPs were coated with citric acid to generate on their surface carboxylic groups useful for subsequent polymer conjugation. The presence of citric acid at the surface reduced the aggregate size as demonstrated from TEM micrograph (figure S1, supporting data) and DLS measurements (table II). The hydrodynamic size of C-MZF NPs was reduced from ~2 μm to 116 nm and the respective polydispersity index from 0.32 to 0.22. It should be noted that core mean diameter is not altered by the treatment as it was reported for NPs smaller than 10 nm [32].

3.2. Polymer conjugation

At the carboxylic groups present on NPs surface, amine groups of the three different polymers were attached by EDC chemistry.

TEM images of the polymer coated NPs are shown in figure 2. The presence of the coating reduces the aggregate size of the uncoated NPs. In the case of Ch MZF NPs, the layer of chitosan that encapsules the NPs is observed as a shadow (figure 2(d)). A reduction of the aggregate size after polymer conjugation was also confirmed by hydrodynamic size values (table 2).

DLS measurements showed hydrodynamic sizes of 95 and 139 nm for PEG and dextran conjugated NPs respectively. In the case of chitosan, this strategy led to the formation of large aggregates (>700 nm, data not shown), for this reason a second strategy was developed. Uncoated MZF NPs were encapsulated in a chitosan shell by ionic gelation technique in the presence of appropriate TPP concentration (1.25 mg ml^{-1}). The final hydrodynamic size was of 299 nm (table 2). Only for the coated particles with the smallest hydrodynamic size (PEG coated), i.e. suitable for intravenous administration, we tested the effect of different concentrations of salt in comparison to the citric coated ones. Slight variations of the hydrodynamic size was observed for the PEG coated sample, from 95 nm up to 140 nm confirming that the colloidal stability is achieved by electrostatic and steric repulsions (figure S2).

The unmodified magnetic NPs precipitated in aqueous suspension at pH 7, according to their isoelectric point that gives a charge around 0 mV at this pH (figure 3). Citric acid molecules provided the stabilization in water at pH 7 via electrostatic repulsions through the negative charge of the carboxylic groups shifting the isoelectric point from 7 to around pH 3. After dextran and PEG conjugation, the isoelectric point did not change significantly but the surface charge at pH 7 was slightly reduced from −24 to −20 and −18 mV respectively (figure 3). Low surface charge of dextran and PEG conjugated NPs at pH 7 (figure 3), demonstrates the effect of PEG and dextran coating on the stabilization of the MNPs through electrostatic and steric repulsions. The Ch-MZF NPs exhibited positive charge at physiological pH and isoelectric point at pH 8. It is known that the chitosan as polymer is deprotonated and not water soluble at pH values above its pK_a (equal to 6.5). However, there are obviously stabilizing ionic forces exerted by TPP, strong enough to hold at elevated pH values and maintain the integrity of the chitosan encapsulated NPs [33].

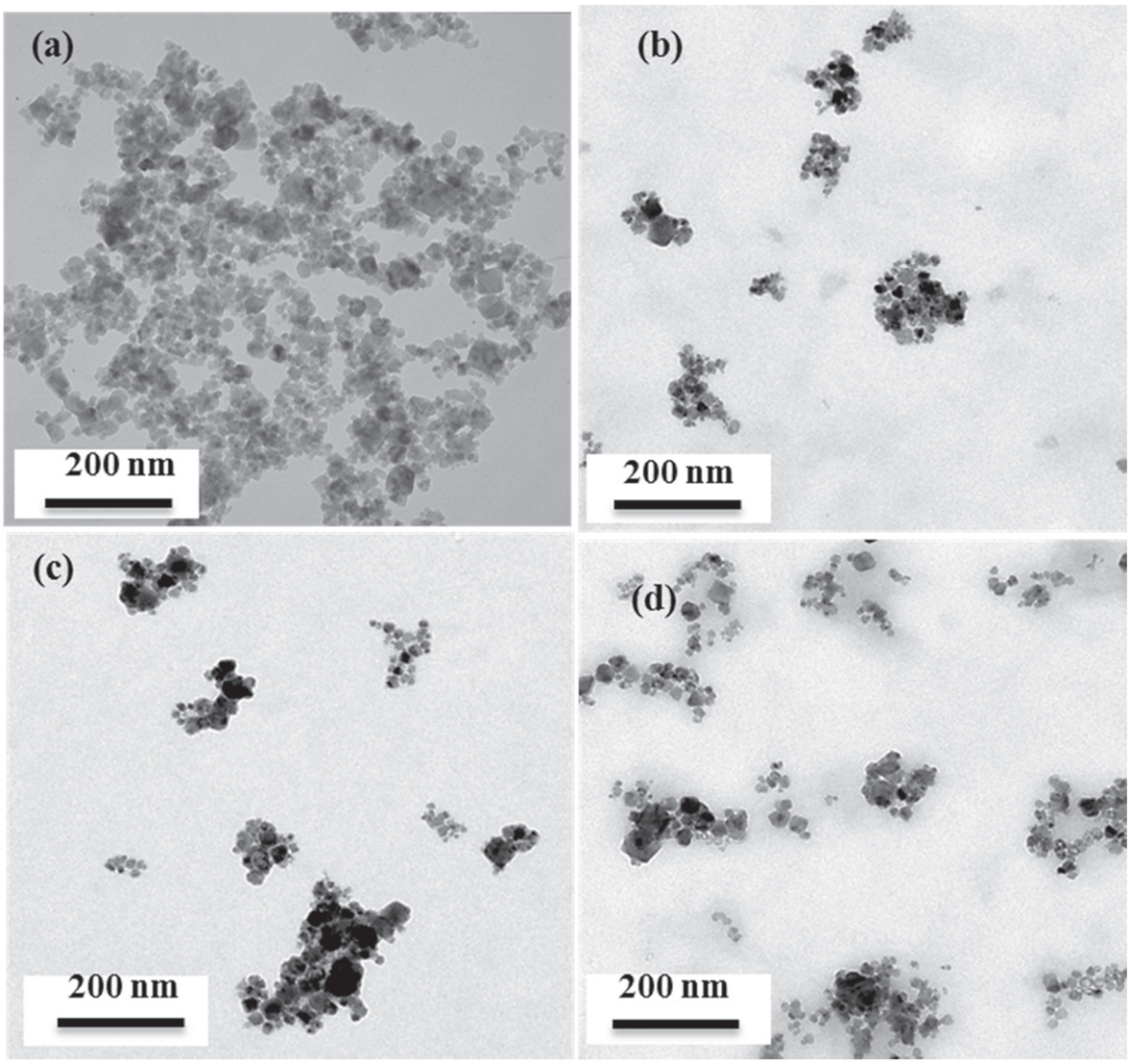

Figure 2. TEM images of (a) naked, (b) P-MZF, (c) D-MZF and (d) Ch-MZF NPs.

Table 2. Colloidal, magnetic and MR relaxometric properties of MZF NPs aqueous suspensions with different surface modification in comparison with commercial products.

Sample	Surface modification	D_H(nm)	PDI	M_s (emu g^{-1})	r_2 (mM s^{-1})	r_1 (mM s^{-1})	r_2/r_1
C-MZF	Citric acid	116	0.22	53.6	132	4	33
P-MZF	Amine PEG	95	0.22	49.2	79.5	3	26.5
D-MZF	Modified dextran	139	0.22	44.8	256.1	2.9	88.3
Ch-MZF[a]	Chitosan	299	0.33	49.9	315.8	5	63.2
Sinerem/Combidex[b]	Dextran	30	*	*	65	9.9	7
Resovist[c]	Carboxydextran	60	*	*	189	9.7	19
VSOP_C184[d]	Citric acid	7	*	*	33.4	14	2
Endorem/Feridex[a]	Dextran	150	*	*	120	10.1	12

*Not measured
[a] Measured at pH = 3.
[b] Guerbet, Advanced Magnetics.
[c] Schering.
[d] Ferropharm.

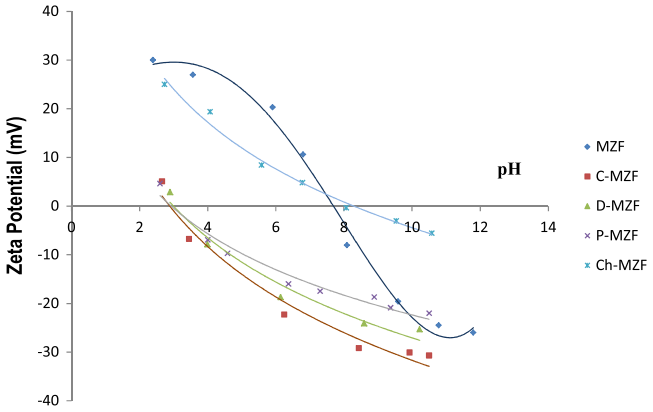

Figure 3. Evolution of zeta potential of naked (MZF), citric acid coated (C-MZF), dextran conjugated (D-MZF), chitosan encapsulated (Ch-MZF) and PEG conjugated (P-MZF) MZF NPs as a function of pH.

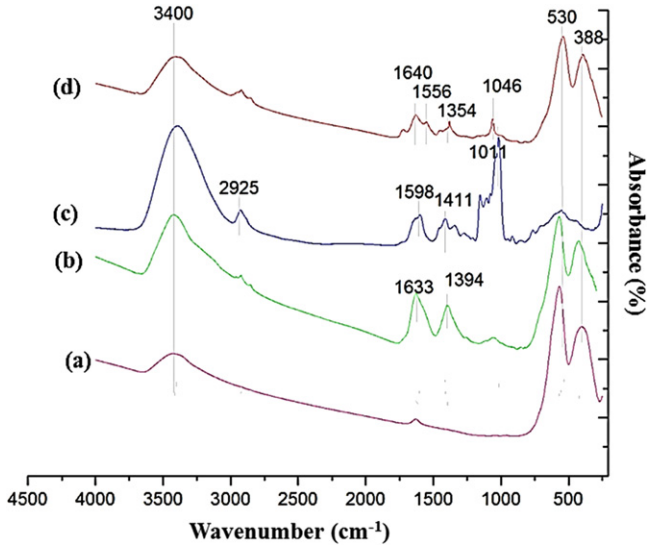

Figure 4. FTIR spectra of (a) naked, (b) citric acid coated (C-MZF), (c) dextran conjugated (D-MZF) and (d) PEG conjugated (P-MZF) MZF NPs.

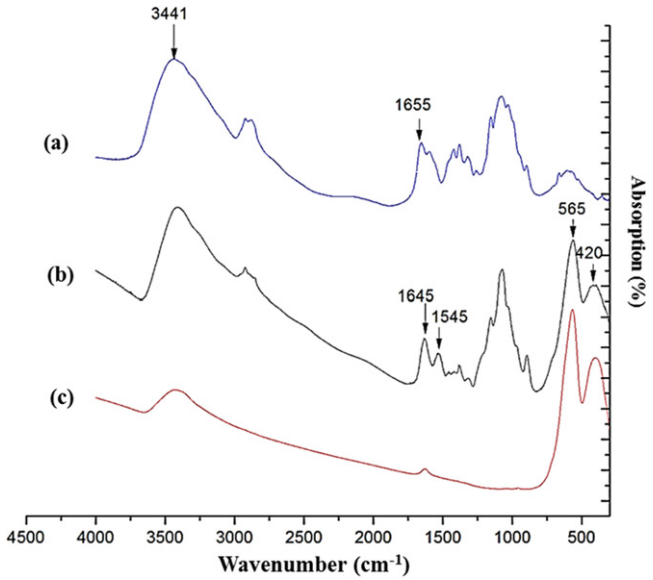

Figure 5. FTIR spectra of (a) chitosan, (b) chitosan-TPP encapsulated NPs and (c) naked NPs.

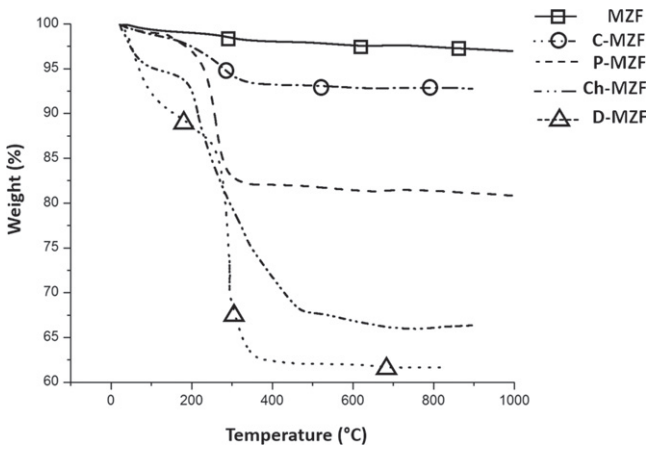

Figure 6. TGA curves for citric acid coated NPs (C-MZF), dextran and PEG conjugated (D-MZF) and chitosan-TPP encapsulated MZF NPs (Ch-MZF) compared with naked ones.

The presence of citric acid and polymers on the NPs surface was also confirmed by FTIR (figures 4, 5) and TGA (figure 6). FTIR spectra of the polymers, PEG and dextran alone are reported in supporting data (figures S3, S4). Figure 4 shows polymer coated NPs (P-MZF and D-MZF NPs) by using the first strategy compared with C-MZF and naked NPs. It is possible to appreciate the presence of the formed amide bond (around 1600 cm^{-1}). In more detail, a broad peak between 3000 and 3500 cm^{-1} (figures 4(a)–(d)) is due to surface OH and NH2 groups [34]. A strong peak at 1627 cm^{-1} shows the C=O vibration (symmetric stretching) from the COOH group of citric acid, so this peak can be assigned to binding of citric acid radicals to the MZF NPs surfaces. The peak in 1394 cm^{-1} indicates the asymmetric stretching of CO from the COOH group [35]. Peaks in the region of 450–600 cm^{-1} are assigned to metal skeleton vibration [36]. After PEG conjugation, some peaks appeared at 1354 and 1046 cm^{-1}, indicating asymmetric and symmetric stretching of C–O–C and out-of-plane bending of the –CH of the PEG chains at 956 cm^{-1} [36, 37]. An intense band appeared between 1000 and 1200 cm^{-1} after surface modification, indicating the presence of aliphatic amines (C–N) and amide carbonyl groups at 1640 and 1556 cm^{-1} [38, 39]. The 2800–2950 cm^{-1} peak in the conjugated samples also indicates successful PEG grafting onto the particle surface [40].

After dextran conjugation, a band appears at 2925 cm^{-1} indicating the asymmetric $-CH_2$ stretching (figure 6(c)). Furthermore, a peak is observed at 1598 cm^{-1} which is characteristic of the R-C(=O)–NHR' amide bond. The formation of an amide bond is indicative of the successful functionalization of C- MZF NPs with aminated dextran molecules. Moreover, vibrational modes at 1411 and

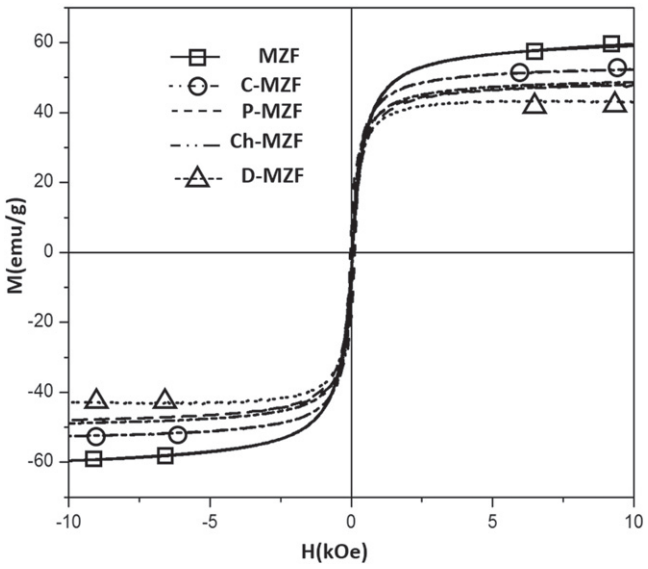

Figure 7. M–H curves at room temperature for naked, chitosan encapsulated NPs (Ch-MZF), citric acid coated (C-MZF), dextran and PEG conjugated NPs (D-MZF, P-MZF).

1016 cm^{-1} are observed representative of $–CH_2$ deformation and C–O groups from the functionalized dextran molecule [13]. The oxide skeleton vibrations which are expected to appear at about 400–600 cm^{-1} are probably covered by the intense dextran peaks. However, the existence of MNPs in the coated NPs is verified by attraction of the particles to a magnet.

The FTIR spectra of chitosan encapsulated NPs (Ch-MZF) in comparison with chitosan and naked NPs are shown in figure 5. A characteristic band at 3441 cm^{-1} is attributed to $–NH_2$ and –OH groups and the band at 1655 cm^{-1} in figure 5(c) is characteristic of the amide band. Whereas, in the FTIR spectrum of Ch-MZF (figure 5(b)), the peak at 1655 cm^{-1} disappears and two new peaks appear at 1645 cm^{-1} and 1545 cm^{-1}. The disappearance of the band could be attributed to the linkage between the phosphoric and amine ions [41]. Appearance of both characteristic peaks of crosslinked chitosan and metal skeleton vibration [36] in figure 5(b) can confirm successful modification of MZF NPs by chitosan.

The amount of coating on the NPs surface was evaluated by TGA (figure 6). TG analyses of C-MZF, P-MZF, Ch-MZF and D-MZF NPs reveal weight losses of 7.2%, 19.7%, 34% and 38% respectively, with respect to 2% for the uncoated ones.

All the samples showed superparamagnetic-like behavior (zero remanence and coercivity) at room temperature (figure 7). Moreover, the presence of the coating led to a slight reduction of the saturation magnetization values.

3.3. Evaluation of NPs as MRI contrast and magnetic hyperthemia agents

To evaluate the effects of surface modified MZF NPs on the contrast in MR imaging, their longitudinal (R_1) and transverse

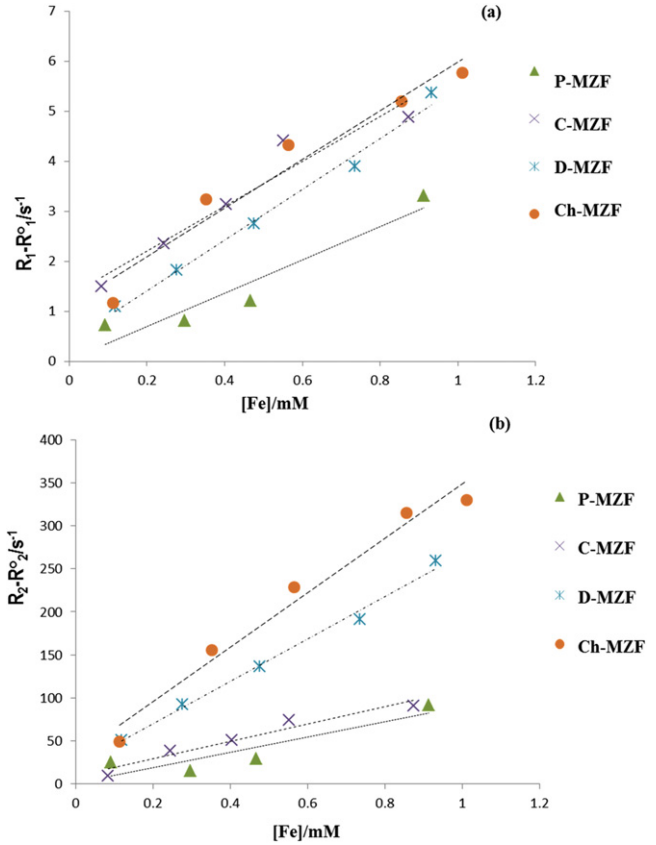

Figure 8. (a), (b) Inversion of the relaxation times as a function of the iron concentration for C-MZF, P-MZF, D-MZF and Ch-MZF NPs.

(R_2) relaxation rates at 1.5 T, typical field strength used currently in clinical MRI, were determined. Table 2 summarizes the measured relaxivity values of r_1 and r_2 which are defined as relaxation rates per concentration of iron (figures 8(a) and (b)).

The conjugation of PEG to C-MZF NPs shows a reduction of r_1 and r_2 values (table 2). The relaxivity reduction produced by the PEG coating can be due to the increased distance of closest approach by the gel's protons to the magnetic cores of the coated particles. The protons diffusing in the vicinity of the particles, therefore, expose a smaller dipolar magnetic field [42]. This reduction effect is applicable for both T_1 and T_2 processes as clearly shown in our results. The reduction in $1/T_1$ is also seen in another study [43] where it is claimed that PEG acts as a barrier for unhindered water diffusion. Furthermore, the proton relaxivity exhibits a strong dependence on the hydrophilicity of coating polymers, suggesting that the accessibility of water to the paramagnetic center contributes greatly to the MRI contrast effect [44]. As a result, particles coated with more hydrophilic ligand as citric acid yields higher proton relaxivity values than particles coated with a less hydrophilic polymer like PEG (table 2).

Dextran conjugated and chitosan encapsulated NPs showed much higher r_2 values (table 2) with respect to C-MZF NPs and also to commercial MRI contrast agents such as Endorem, and Resovist, both prepared by coprecipitation method and with hydrodynamic sizes of 150 and 60 nm,

Table 3. SARs values of chitosan and dextran MZF NPs compared to citrate capped ones and fatty acid coated $MnFe_2O_4$ NPs.

Sample name	Coating	Frequency (kHz)	SAR ($W\,g^{-1}$)
C-MZF	Citric acid	215	17
Ch-MZF	Chitosan	215	50
D-MZF	Dextran	215	48
$MnFe_2O_4$ NPs [31]	Fatty acid	300	21

respectively [22]. r_2 values $<120\,mM^{-1}\,s^{-1}$ are usually obtained for particles synthesized by coprecipitation and also for particles with mean size of 15 nm [45]. The magnetic moment in iron oxide based NPs is due to the localized electron density and hence strongly depends on the degree of crystallographic order [45]. MZF NPs are characterized by an improved crystallinity with respect to commercial products because of their synthesis method that was performed at relatively high temperature and pressure conditions [41, 46]. Moreover, the substitution of Mn and Zn elements into ferrite structure is important to increase saturation magnetization of magnetic core [47]. These, in conjunction with the smaller core size and higher polydispersity of Endorem and Resovist explain the relatively higher relaxivities of our samples. This is a clear advantage for use in MRI imaging, since the dose can be reduced and technique sensitivity can be increased. Moreover, higher r_2 values of chitosan encapsulated NPs in respect of dextran conjugated ones can be related to its lower shielding effect of the coating layer (lower weight loss percent as previously mentioned in TGA results) and the aggregation state of the NPs inside the polymeric coatings. Those high relaxivity values also demonstrate that the magnetic properties of the particles were preserved during the coating process. Generally, the non-magnetic coating layer shields the protons from the magnetic particles and therefore reduces T_1 and T_2 relaxation efficiency. The alteration of the magnetic particles during the coating process can also produce a reduction of the relaxivities. However, further factors, such as the time spent near the particle, have to be taken into account, especially for T_1 [42].

Magnetic NPs can serve as colloidal mediators for heat generation by converting their magnetic into thermal energy in the presence of an external AC magnetic field. With this aim, we have chosen NPs coated with two different strategies (Dextran and Chitosan) to evaluate their application in magnetic hyperthermia. These samples have also shown the highest r_2 values and could be good candidates to be used as theragnostic agents.

SARs values for Ch-MZF and D-MZF NPs calculated from equation (2) were 50 and 48 $W\,g^{-1}$ respectively (table 3). These values are higher than citrate capped iron oxide NPs (16.74 $W\,g^{-1}$) measured at 215 kHz [27] and also fatty acid coated $MnFe_2O_4$ NPs (21 $W\,g^{-1}$) values measured at 300 kHz [31]. In more detail, SAR values of polymer coated NPs have been tripled with respect to C-MZF due to the cooperative behavior of the particles (dipolar interactions) inside the aggregates [48]. These data are important because a high SAR is necessary for efficient hyperthermia therapy with a minimal dose of MNPs in the body.

3.4. NPs evaluation in HeLa cells

Among the prepared polymer coated NPs, P-MZF NPs showed suitable hydrodynamic size (smaller than or about 100 nm at pH of 7) for intravenous administration. For this reason these NPs were subjected to investigation in HeLa (human cervical adenocarcinoma) cells, compared with C-MZF NPs used as blank.

In vitro analysis on cell cultures allows us to gain insights on the nanoparticle-cell interactions at the cellular level. Cell cultures have become the first indispensable step to evaluate nanoparticle effectiveness and safety and are used for pre-screening nanomaterials before *in vivo* analysis.

This cell line is commonly used for cytotoxicity evaluation in different research fields, including nanomaterials, and therefore it provides a good basis for comparison [1, 10].

Intracellular uptake of nanoparticles was detected under bright light microscopy after Prussian blue staining. HeLa cells incubated with citric acid and PEG-coated NPs for 24 h at two different concentrations (0.1 and 0.2 mg Fe ml^{-1}) showed efficient internalization (100% cells were labelled) and concentration dependent uptake. Importantly, our results highlight the essential role of appropriate PEG-coated iron oxide nanoparticles in order to allow cell labeling which is an essential property for MRI studies. Recently, Pelaz *et al* have reported that uptake of NPs by 3T3 fibroblasts was reduced to around 10% upon PEGylation with PEG chains of 10 kDa [49].

Moreover, cell morphology with NPs internalized was flat and well-spread, similar to control cells, indicating that NP accumulation into the cells did not induce cytotoxic effects (figure 9). Likewise, no alteration in nuclei nor any micronucleus, that might indicate possible genotoxic damage, were found after NPs administration and incubation. It is well known that changes in cell morphology are indicative of cell health and can be used to identify potential cytotoxicity in response to toxic agents, including oxide NP and asbestos, prior to alterations in metabolism or proliferation [50].

To corroborate this result, Alamar Blue cell viability assay was so performed. Citric acid and PEG-coated NPs were incubated at the same conditions indicated before and cytotoxicity was analyzed immediately after NP incubation or after 48 h without NPs (figure 10).

As can be seen in figure 10 Alamar Blue assay results indicated that all the analyzed samples were not cytotoxic even at the highest concentration tested (0.2 mg Fe ml^{-1}), which exceeds by one order of magnitude the concentrations of conventional iron-oxide-based-MRI contrast agents typically used in mice (1–20 mg kg^{-1}) [46]. In the case of C-MZF NPs, cell viability decreased slightly after 24 h incubation, but after 48 h without NPs it was recovered. Likewise, cell viability increased after coating by PEG (from 95.09 $\pm$ 3.05% to 99.38 $\pm$ 1.88%).

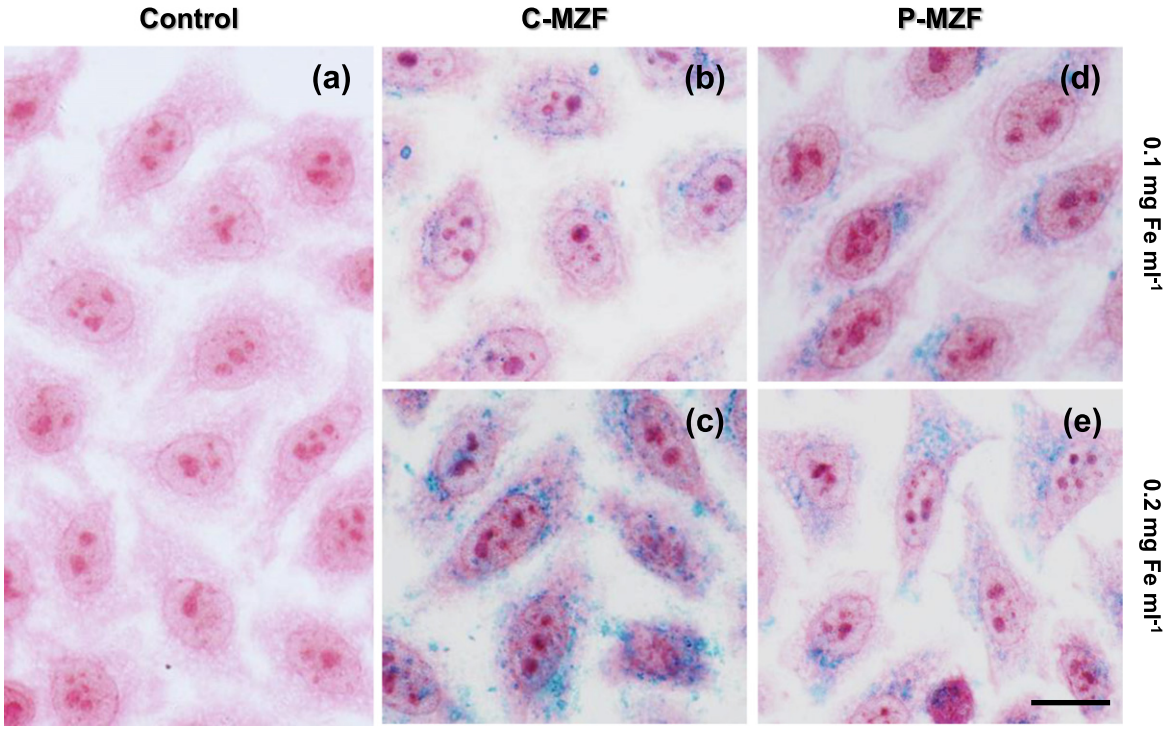

Figure 9. Internalization and uptake of MNP (blue spots) inside HeLa cells stained with Prussian blue reaction for iron oxide detection after 24 h of incubation. (a) Untreated control cells. (b) Cells incubated with C-MZF at 0.1 or (c) 0.2 mg Fe ml^{-1}. (d) Cells incubated with P-MZF at 0.1 or (e) 0.2 mg Fe ml^{-1}. Scale bar = 10 μm.

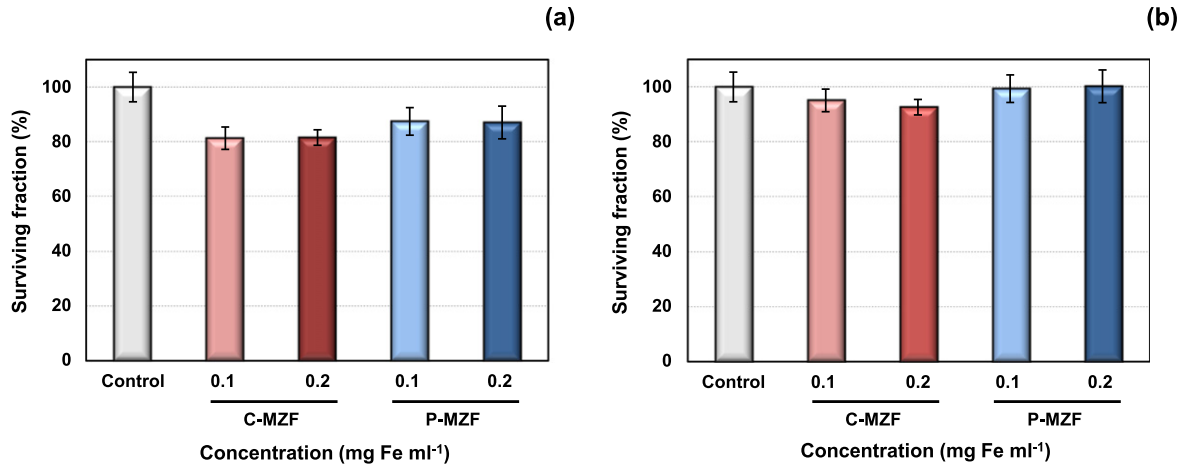

Figure 10. Cell viability of HeLa cells treated with various concentrations of C-MZF (red), and P-MZF (blue) NPs analyzed after 24 h of incubation at (a) 0 and (b) 48 h post-incubation in comparision with control (white color) measured by Alamar Blue assay.

4. Conclusions

Crystalline MZF NPs with core size of 14 nm were successfully obtained and subsequently modified with three biocompatible polymers, PEG, dextran and chitosan, to improve their colloidal properties at physiological pH. Two different coating strategies to obtain a strong shell around the NPs have been approached, one based on the formation of an amide bond and the other on the NPs encapsulation. Both methods have permitted obtaining biocompatible coated NPs stable in water at pH 7 and useful for biomedical applications.

In particular relaxometric properties of PEG, dextran and chitosan coated NPs, were investigated. An important finding is that the measured proton relaxation rates strongly depend on the coating layer hydrophilicity. D-MZF and Ch-MZF NPs have shown high r_2 values demonstrating good MRI contrast agents. PEG coating reduces both T_1 and T_2 relaxation enhancement due to increased distance of water spins closest to the magnetic moment. Furthermore, PEG coating reduces particle aggregation by increasing inter-particle spacing. However the values of r_2/r_1, which are also indicative of contrast agent effectiveness, were high for all samples, and

higher than reported values for Endorem, Sinerem and VSOP-C184. Higher magnetic moment of these samples due to the substitution of Mn and Zn elements into ferrite structure, in conjunction with the smaller core size and higher poly-dispersity of Endorem and Resovist, explain the higher relaxivities of our samples.

Dextran conjugated and chitosan encapsulated NPs have also shown remarkable heating effect during the application of an alternating magnetic field which makes them attractive for biomedical heating applications, such as magnetic fluid hyperthermia for cancer therapy. These coatings could be very interesting for the use of MZF NPs as theragnostic agents.

Cytotoxicity of PEG conjugated NPs with an hydro-dynamic size about 100 nm suitable for intravenous admin-istration, was investigated. These particles led to high cell viability resulting in good candidates for *in vivo* applications as drug/biomolecule carriers.

Acknowledgments

This work was supported by the Isfahan University of Technology, Iran and partially supported by the European Union (EU-FP7MULTIFUN project, ref. 246479, MAT2014-52069-R and S2013/MIT-2850). We want to thank ICMM technicians for chemical-physical characterization of the samples (ICP, FT-IR and TGA).

References

[1] Veintemillas-Verdaguer S *et al* 2015 *Nanotechnology* **26** 135101
[2] Psimadas D, Baldi G, Ravagli C, Franchini M C, Locatelli E, Innocenti C, Sangregorio C and Loudos G 2014 *Nanotechnology* **25** 025101
[3] Yang S H *et al* 2013 *Nanotechnology* **24** 475103
[4] Shahbazi-Gahrouei D, Abdolahi M, Zarkesh S H, Laurent S, Sermeus C and Gruettner C 2013 *Biomed. Res. Int.* **2013** 349
[5] Mazarío E, Herrasti P, Morales M P and Menéndez N 2012 *Nanotechnology* **23** 355708
[6] Lee J H *et al* 2007 *Nat. Med.* **13** 95
[7] Seo W S *et al* 2006 *Nat. Mater.* **5** 971
[8] Hejase H, Hayek S S, Qadri S and Haik Y 2012 *J. Magn. Magn. Mater.* **324** 3620
[9] Jang J T, Nah H, Lee J H, Moon S H, Kim M G and Cheon J 2009 *Angew. Chem. Int. Ed.* **48** 1234
[10] Ruiz A, Salas G, Calero M, Hernández Y, Villanueva A, Herranz F, Veintemillas-Verdaguer S, Martínez E, Barber D F and Morales M P 2013 *Acta Biomater.* **9** 6421
[11] Mornet S, Portier J and Duguet E 2005 *J. Magn. Magn. Mater.* **293** 127
[12] Latorre-Esteves M, Cortés A, Torres-Lugo M and Rinaldi C 2009 *J. Magn. Magn. Mater.* **321** 3061
[13] Creixell M, Herrera A P, Latorre-Esteves M, Ayala V, Torres-Lugo M and Rinaldi C 2010 *J. Mater. Chem.* **20** 8539
[14] Patil R M, Shete P B, Thorat N D, Otari S V, Barick K C, Prasad A, Ningthoujam R S, Tiwale B M and Pawar S H 2014 *J. Magn. Magn. Mater.* **355** 22
[15] Qu J, Liu G, Wang Y and Hong R 2010 *Adv. Powder Technol.* **21** 461
[16] Hritcu D, Popa M I, Popa N, Badescu V and Balan V 2009 *Turk. J. Chem.* **33** 785
[17] McBain S C, Griesenbach U, Xenariou S, Keramane A, Batich C D, Alton E and Dobson J 2008 *Nanotechnology* **19** 405102
[18] Duan H W, Kuang M, Wang X X, Wang Y A, Mao H and Nie S M 2008 *J. Phys. Chem.* C **112** 8127
[19] Mahmoudi M, Simchi A and Imani M 2010 *J. Iran Chem. Soc.* **7** S1
[20] Tartaj P, Morales M P, Veintemillas-Verdaguer S, Gonzalez-Carreno T and Serna C J 2006 *Handbook of Magnetic Materials* (Amsterdam: Elsevier)
[21] Veiseh O, Gunn J W and Zhang M 2010 *Adv. Drug Deliv. Rev.* **62** 284
[22] Laurent S, Forge D, Port M, Roch A, Robic C, Elst L V and Muller R N 2008 *Chem. Rev.* **108** 2064
[23] Marciello M, Connord V, Veintemillas-Verdaguer S, Andrés Vergés M, Carrey J, Respaud M, Serna C J and Morales M P 2013 *J. Mater. Chem.* B **1** 5995
[24] Yu M, Huang S, Yu K J and Clyne A M 2012 *Inter. J. Mol. Sci.* **13** 5554
[25] Zahraei M, Monshi A, Morales M P, Shahbazi-Gahrouei D, Amirnasr M and Behdadfar B 2015 *J. Magn. Magn. Mater.* **393** 429
[26] Costo R, Bello V, Robic C, Port M, Marco J F, Morales M P and Veintemillas-Verdaguer S 2012 *Langmuir* **28** 178
[27] Cheraghipour E, Javadpour S and Mehdizadeh A R 2012 *J. Biomed. Sci. Eng.* **5** 715
[28] Marciello M, Bolivar J M, Filice M, Mateo C and Guisan V 2013 *Biomacromolecules* **14** 602
[29] Cullity B D 1996 *Elements of X-ray Diffraction* vol 1 2nd edn (Boston, MA: Addison-Wesley)
[30] Roca A G, Veintemillas-Verdaguer S, Port M, Robic C, Serna C J and Morales M P 2009 *J. Phys. Chem.* B **113** 7033
[31] Giri J, Pradhan P, Sriharsha T and Bahadur D J 2005 *Appl. Phys.* **97** 10Q916
[32] Hilger I and Kaiser W A 2012 *Nanomedicine* **7** 1443
[33] Käuper P and Forrest M 2006 *14th Int. Workshop on Bioencapsulation (Switzerland)*
[34] Lattuada M and Hatton T 2007 *Langmuir* **23** 2158
[35] Behdadfar B, Kermanpur A, Sadeghi-Aliabadi H, Morales M P and Mozaffari M 2012 *J. Magn. Magn. Mater.* **324** 2211
[36] Amstad E, Gillich T, Bilecka I, Textor M and Reimhult E 2009 *Nano Lett.* **9** 4042
[37] Amici J, Celasco E, Allia P, Tiberto P and Sangermano M 2011 *Macromol. Chem. Phys.* **212** 411
[38] Kohler N, Sun C, Fichtenholtz A, Gunn J, Fang C and Zhang M 2006 *Small* **2** 785
[39] Sun C *et al* 2010 *ACS Nano* **4** 2402
[40] Barrera C, Herrera A and Rinaldi C 2009 *J. Colloid. Interface Sci.* **329** 107
[41] Bhumkar D R and Pokharkar V B 2006 *AAPS Pharm. Sci. Tech.* **7** E138
[42] Issa B, Qadri S, Obaidat I M, Bowtell R W and Haik Y 2011 *Magn. Reson. Imaging* **34** 1192
[43] Bulte J, Cuyper M, Despres D and Frank J A 1999 *J. Magn. Magn. Mater.* **194** 204
[44] Di Marco M, Guilbert I, Port M, Robic C, Couvreur P and Dubernet C 2007 *Int. J. Pharma.* **331** 197
[45] Amiri H, Bustamante R, Millán A, Silva N J, Piñol R, Gabilondo L, Palacio F, Arosio P, Corti M and Lascialfari A 2011 *Magn. Reson. Med.* **66** 1715
[46] Huang J, Bu L, Xie J, Chen K, Cheng Z, Li X and Chen X 2010 *ACS Nano* **4** 7151

[47] Cullity B D and Graham C D 1996 *Introduction to Magnetic Materials* 2nd edn (Hoboken, NJ: Wiley)
[48] Coral D F, Mendoza Zelis P, Marciello M, Morales M P, Craievich A, Francisco H, Sanchez F H and Fernandez van Raap M B 2016 *Langmuir* **32** 1201
[49] Pelaz B, del Pino P, Maffre P, Hartmann R, Gallego M, Rivera-Fernandez S, de la Fuente J M, Nienhaus G U and Parak W J 2015 *ACS Nano* **9** 6996
[50] Brunner T J, Wick P, Manser P, Spohn P, Grass R N, Limbach L K, Bruinink A and Stark W J 2006 *Environ. Sci. Technol.* **40** 4374